Received: 21 December 2019 | Revised: 9 March 2020 | Accepted: 12 March 2020

DOI: 10.1002/osp4.417

ORIGINAL RESEARCH ARTICLE

Obesity Science and Practice Open Access WILEY

Differences in brain structure and function in children with the *FTO* obesity-risk allele

Claudia Lugo-Candelas[1,2] | Yajing Pang[3] | Seonjoo Lee[2,4] | Jiook Cha[1,2] | Susie Hong[2] | Lisa Ranzenhofer[1,2] | Rachel Korn[1,2] | Haley Davis[1,2] | Hailey McInerny[1] | Janet Schebendach[1,2] | Wendy K. Chung[5,6] | Rudolph L. Leibel[5,7] | B. Timothy Walsh[1,2] | Jonathan Posner[1,2] | Michael Rosenbaum[2] | Laurel Mayer[1,2]

[1]Department of Psychiatry, Columbia University Irving Medical Center, New York, New York, USA

[2]New York State Psychiatric Institute, New York, New York, USA

[3]The Clinical Hospital of Chengdu Brain Science Institute, MOE Key Lab for Neuroinformation, University of Electronic Science and Technology of China, Chengdu, China

[4]Department of Biostatistics, Mailman School of Public Health, Columbia University Irving Medical Center, New York, NY

[5]Department of Pediatrics, Columbia University Irving Medical Center, New York, New York, USA

[6]Department of Medicine, Columbia University Irving Medical Center, New York, New York, USA

[7]Naomi Berrie Diabetes Center, Columbia University Irving Medical Center, New York, New York, USA

Correspondence
Claudia Lugo-Candelas, PhD, Department of Psychiatry, Columbia University Irving Medical Center/New York State Psychiatric Institute, 1051 Riverside Dr., New York, NY 10032, USA.
Email: claudia.lugo@nyspi.columbia.edu

Funding information
National Institute of Diabetes and Digestive and Kidney Diseases, Grant/Award Numbers: 5P30DK026687, R01-DK52431, R56/R01 DK097399; National Institutes of Health Clinical and Translational Science Award (CTSA), Grant/Award Number: UL1 TR000040

Summary

Objective: Noncoding alleles of the fat mass and obesity-associated (*FTO*) gene have been associated with obesity risk, yet the underlying mechanisms remain unknown. Risk allele carriers show alterations in brain structure and function, but previous studies have not disassociated the effects of genotype from those of body mass index (BMI).

Methods: Differences in brain structure and function were examined in children without obesity grouped by their number of copies (0,1,2) of the FTO obesity-risk single-nucleotide polymorphism (SNP) rs1421085. One hundred five 5- to 10-year-olds (5th–95th percentile body fat) were eligible to participate. Usable scans were obtained from 93 participants (15 CC [homozygous risk], 31 CT [heterozygous] and 47 TT [homozygous low risk]).

Results: Homozygous C allele carriers (CCs) showed greater grey matter volume in the cerebellum and temporal fusiform gyrus. CCs also demonstrated increased bilateral cerebellar white matter fibre density and increased resting-state functional connectivity between the bilateral cerebellum and regions in the frontotemporal cortices.

Conclusions: This is the first study to examine brain structure and function related to *FTO* alleles in young children not yet manifesting obesity. This study lends support to the notion that the cerebellum may be involved in *FTO*-related risk for obesity, yet replication and further longitudinal study are required.

KEYWORDS

children, *FTO*, imaging, obesity

1 | INTRODUCTION

Since 2007, a large body of literature has shown that polymorphisms in noncoding regions (primarily the first intron) of the fat mass and obesity-associated (*FTO*) gene are associated with higher body mass index (BMI) and risk for obesity.[1] However, the mechanisms underlying the association between *FTO* and obesity are not well understood. Children without obesity, who carry risk alleles, show increased food intake.[2] However, energy expenditure—adjusted for body composition—does not differ by *FTO* genotype.[3] Given that *FTO* is highly expressed throughout the brain, examining brain structure and function across genotypes is of paramount importance to understanding mechanisms by which *FTO* might affect adiposity.

An increasing number of studies have begun to describe brain differences correlated with *FTO* genotypes.[4] Overall lower brain volumes,[5] as well as specific volumetric reductions in the nucleus accumbens,[6] have been documented in *FTO* risk allele carriers relative to noncarriers. Further, white matter (WM) microstructure abnormalities have been detected in risk allele carriers in the anterior thalamic radiations and the accumbofrontal fasciculus.[7] However, one study failed to document differences in WM integrity across genotypes.[8] Functional MRI (fMRI) studies of *FTO* genotypes have focused on regional brain activity during food viewing tasks; however, findings have been inconsistent. Some studies report that adult risk allele carriers show increased activity[9,10] in impulsivity-related neural circuits in response to food images, yet others find decreased activity,[11] and still, others find no group differences at all.[12] Risk and nonrisk allele groups also differ in their neural responses to meal consumption and glucose ingestion, but again, study findings differ in direction.[12,13] The brain regions implicated have also varied across studies and include the posterior cingulate, cuneus, precuneus, putamen, prefrontal cortex, hypothalamus, substantia nigra, hippocampus, ventral striatum and medial orbitofrontal cortex. Only one resting fMRI study has been published, and although no *FTO* genotype-related differences were detected, a risk genotype by anxious temperament interaction was associated with increased connectivity in regions of the default mode, sensorimotor and salience resting-state networks.[14]

Taken together, studies suggest that segregation for *FTO* obesity-risk alleles is associated with structural and functional alterations in brain regions responsible for reward processing, inhibitory control and goal-directed behaviour. However, differences in study designs preclude strong inferences regarding the validity of these associations. Studies have varied in both which single-nucleotide polymorphisms (SNPs) are examined, as well as the cohort's ethnic and racial composition, which is important to consider together, as associations between SNPs and adiposity vary across ethnicities. Furthermore, some studies restrict samples to average weight,[10] whereas others include overweight or individuals with obesity.[9] Because adiposity, weight gain and diet affect brain structure and function,[15] cohorts including adults with significant BMI differences across genotypes cannot differentiate genotypic effects from those of adiposity per se. Only one study in children exists and documented greater intensity of responses to food stimuli reward processing systems in risk allele carriers (examining rs9939609 SNP[16]). However, children in this sample already displayed significant increases in BMI across *FTO* genotypes. On the other hand, studies that focus on adult samples with exclusively nonobese BMIs may introduce sampling bias by including a select group of participants who, despite carrying risk alleles, are able to avoid weight gain even through adulthood. Such studies may be identifying compensatory mechanisms, rather than genetic vulnerabilities.

The *FTO* genotype-related mechanisms leading to weight gain are thus better examined in young children who are at genetic risk for obesity but do not yet manifest obesity. The present study examined differences in brain structure and function between *FTO* SNP rs1421085 allele carriers in 5- to 10-year-old children without obesity. Based on prior literature, it was predicted that risk allele carriers would demonstrate structural and functional alterations in brain regions responsible for reward processing and inhibitory control, including the default mode, sensorimotor and salience resting-state networks. Given the inconsistencies in previous findings and study designs, no directional hypotheses were made.

2 | METHODS

2.1 | Participants

One hundred ninety-nine children between the ages of 5 and 10 were enrolled in the parent study.[2] As part of the parent study, the relationship between *FTO* rs9939609 and total calorie intake was examined across a subgroup of 122 children—documenting significant association between *FTO* "dose" (number of copies of SNP rs9939609, adjusting for body mass) and total intake, but not macronutrient preference, energy density or diet variety.[2] Participants were included in the parent study if they were between the ages of 5 and 10, generally healthy and less than 95th body fat percentile (recruitment procedure are detailed elsewhere[2]). In the course of the parent study, data were published suggesting that SNP rs1421085 addressed certain ancestry limitations inherent to SNP rs9939609.[17] Thus, in the present study, rs1421085 SNP was examined as it has been related to adiposity across samples of varying racial ancestry.[18]

Exclusion criteria for the present study included MRI contraindications (i.e., irremovable metal in the body), reporting medical conditions relevant to eating behaviour (e.g., diabetes and eating disorders) or use of any medications that impact eating behaviour (e.g., anorexiants, catecholamines and corticosteroids). One hundred five children were interested and eligible to complete an MRI scan, and of these, nine were unable to complete scanning procedures (three unable to acclimate to the scanner and removed before any scanning was initiated and six asked to terminate the scans prematurely [stomach hurt (N = 2), ears hurt (N = 2), head hurt (N = 1), and bored (N = 1)]). Imaging data from all remaining 96 participants were visually inspected by trained research staff (CLC and YP). In this step, it was determined that three participants had motion-related imaging artefacts across all modalities deemed too severe to be utilized (e.g., images were completely blurry/choppy).

The scanned sample thus consisted of 93 children (50 girls and 43 boys). Generally consistent with Hardy–Weinberg expectations, 15 (16%) were CC, 31 (33%) were CT and 47 (50%) were TT. In the *FTO* SNP rs1421085, CC genotypes are considered at-risk genotypes for increased adiposity compared with TTs.[19] The New York State Psychiatric Institute/Columbia University Institutional Review Board approved all procedures. Child participants provided assent, and parents/guardians provided consent prior to study participation.

2.2 | Procedures

The study was conducted over the course of two visits. In the first, participants and parent/guardians completed clinical and medical interviews. Children's height, weight and body composition were measured, and saliva was collected for DNA isolation. Children eligible for MRI procedures returned for a second visit. The night prior to the second study visit, children were asked not to eat or drink (except water) past 10 PM. In the morning, upon arrival to the clinic, children were provided a standardized breakfast adjusted for calculated energy expenditure based on age, gender and weight prior to the MRI scan.

2.3 | Genotyping and *FTO* obesity risk group definition

Saliva was collected, and DNA was extracted using DNA Genotek™ kit. Children were genotyped for the C/T rs1421085 SNP of *FTO* by pyrosequencing (PSQ96 Biotage, LLC. Westborough, MA). PCR reactions consisted of 6 pmol of each of the forward and reverse primer, 0.75-U GoTaq, 1xGoTaq buffer, 0.2-mM dNTP's and 50 ng of genomic DNA in a 30-μλ reaction volume for 35 cycles at an annealing temperature of 50°C.

2.4 | MRI acquisition and preprocessing

Structural and functional brain images were acquired on a GE Signa 3T whole-body scanner (MR 750; GE Healthcare) with a 32-channel head coil. T1-weighted structural MRI, diffusion-weighted images and functional images were obtained from 96 participants. For the T1-weighted structural scans, the imaging parameters were 3D BRAVO (BRAin VOlume imaging) sequence, voxel size $1 \times 1 \times 1$ mm^3, dimensions $256 \times 256 \times 176$, FOV 25.6 cm, TI (inversion time) 450 ms, 12° flip angle, S/I. For diffusion, MRI parameters were as follows: voxel size $0.9375 \times 0.9375 \times 2.49997$ mm^3; dimensions $256 \times 256 \times 56$; field of view (FOV) 24 cm; slices 60, TR/TE 8500/minimum, flip angle 90°, and three images without diffusion weighting (b0) and 25 images with diffusion weighting along noncollinear directions (b = 1000 s m^{-2}). For resting state MRI, echoplanar images with the following parameters were collected: (R/L, TR = 2000 ms, TE = 30 ms, 90° flip angle, single excitation per image, slice thickness 3.5 mm, 24×24 cm FOV, 64×64 matrix, 34 slices, interleaved, bottom-up) with an effective resolution of $3.75 \times 3.75 \times 3.5$ mm and whole-brain coverage. Two runs of 155 volumes were obtained for each participant. Prior to preprocessing, all images first underwent visual inspection. By MRI modality, 91 had usable T1-weighted scans, 89 had diffusion-weighted images and 73 had resting-state functional images.

T1 scans underwent voxel-based morphometry (VBM). Images underwent nonparametric non-uniform intensity normalization (N3) correction.[20] Brain extraction was performed with Brain Extraction Tool (BET).[21] Spatial normalization, segmentation, template generation and smoothing were done using the Diffeomorphic Anatomical Registration Through Exponentiated Lie (DARTEL) algebra toolbox in SPM12.[22] Images were smoothed using a 6-mm full-width-half-maximum (FWHM) kernel. After each step, a trained research assistant, blind to group assignment, visually inspected the quality of output. Five participants were dropped from the analyses (two had excessive motion artefacts and three failed to obtain acceptable segmentation).

Diffusion-weighted scans underwent fixel-based morphometry (FBM). First, a trained research assistant examined every Diffusion weighted imaging(DWI) volume for severe artefacts. Images containing eight or more rejected volumes were excluded; seven participants were excluded. FBM is a novel method that incorporates measures of fibre density and fibre-bundle morphology (cross section) to examine WM integrity more comprehensively.[23] The FBM pipeline was run in MRtrix3, and details can be found at https://mrtrix.readthedocs.io/en/latest/index.html. Fibre orientation distributions (FODs) are estimated implementing a constrained spherical deconvolution (CSD). A study specific FOD template is generated, and participant's FOD images were registered to the group template. Next, a WM template analysis fixel mask is created by segmenting fixels from the FOD template (Figure 1). This fixel mask then delineates the fixels that will be used in statistical analyses.[24] Fibre density (FD), fibre cross section (FC), and a combined measure of the two (fibre density and cross section [FDC]) were then computed. Nonparametric permutation testing fixel-based analysis were utilized to assess group differences.

Functional images were preprocessed using the ICA-based strategy for Automatic Removal of Motion Artifacts (ICA-AROMA) and seed-based analyses using the CONN toolbox. First, a trained researcher (YP) visually examined every run and selected the one with the fewest motion for each participant. ICA-AROMA[25] was then used to remove motion artefacts from the data. Only participants with at least one run with ≤0.5 mm mean framewise displacement (FD[26]) were included. From the 96 participants scanned, 23 were excluded for excessive motion, and all participants in the resulting sample had runs with ≤0.3. Mean FD analyses showed that head motion did not vary across (CC [m = 0.087 ± 0.069 mm; range = 0.03–0.31 mm), CT [m = 0.082 ± 0.062 mm; range = 0.03–0.27 mm] and TT [m = 0.089 ± 0.070 mm; range = 0.02–0.30 mm]) groups ($F_{2,70}$ = 0.70, p = 0.93). Motion-corrected images were then coregistered with an anatomical scan, normalized, scrubbed and smoothed with a Gaussian kernel of 6-mm FWHM in CONN v.18.b.[27] Temporal band-pass filtering (0.008–0.09 Hz) was applied. Figure 2 provides details on head motion.

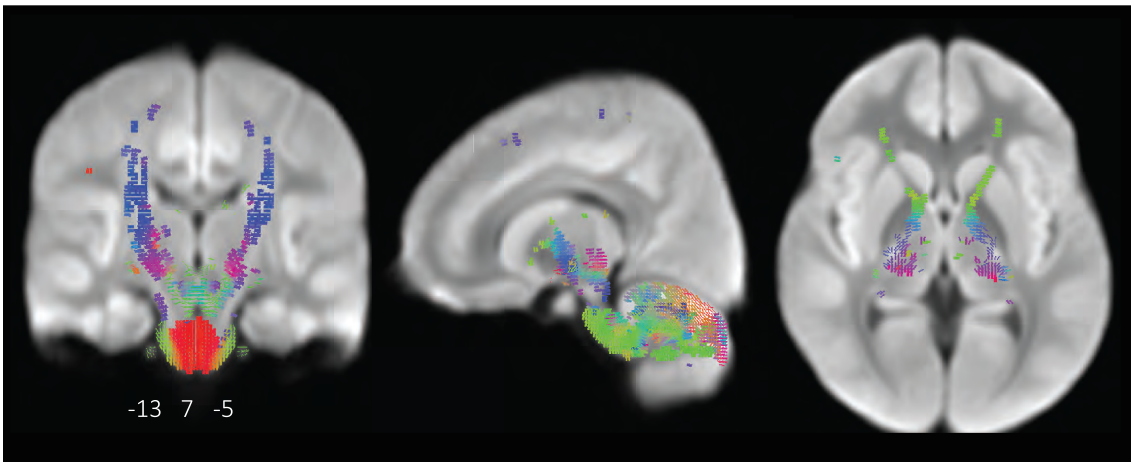

FIGURE 1 Study specific fibre orientation distributions (FODs) analysis mask. Study-specific fibre density, fibre cross section, and fibre density and cross-sectional analysis mask. Colours indicate the orientation of the FOD/fixel orientation (red: left–right, blue: inferior–superior, green: anterior–posterior)

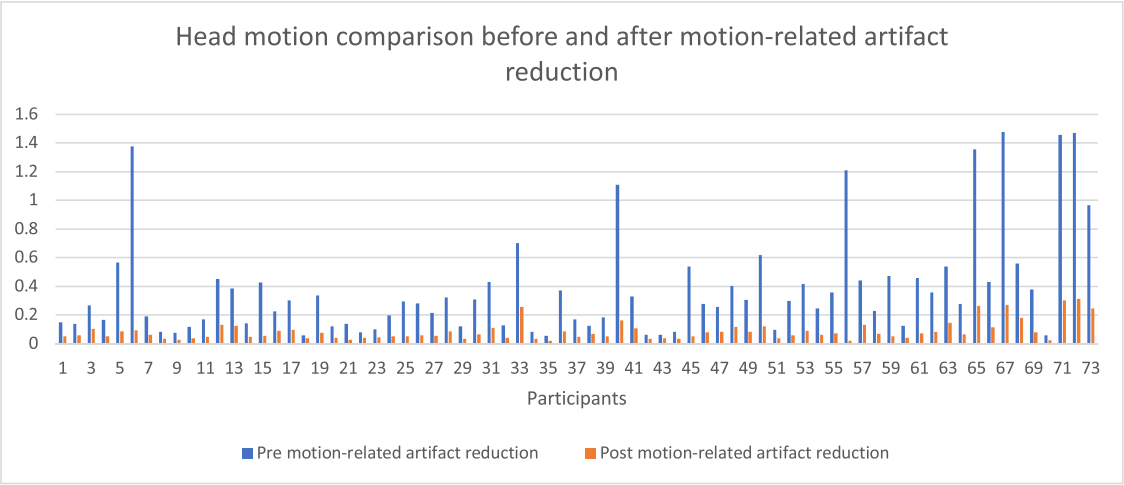

FIGURE 2 Head motion comparison before and after motion-related artefact reduction. Participant's average framewise displacement (FD) measurement before and after preprocessing after motion-related artefact removal included using the ICA-based strategy for Automatic Removal of Motion Artifacts (ICA-AROMA) as well as scrubbing in CONN

2.5 | Statistical analyses

In line with prior research, group comparisons between homozygous allele carriers (CC vs. TT) were conducted.[7,9,13,14] However, given that MRI studies have found evidence for additive,[5,6,12] recessive[10,28] and dominant[4,11] *FTO* effects, differences were also investigated between the homozygous groups and heterozygous allele carriers (CC vs. CT and CT vs. TT). All analyses included the following covariates: child sex, age at scan and BMI. Given that volumetric differences have been most widely investigated in the existing literature, VBM grey matter (GM) analyses were selected as the primary analyses of interest. To be maximally stringent, nonparametric permutation testing was used to determine statistical significance in VBM analyses. Type 1 error was controlled for using conditional Monte Carlo permutation testing with 10 000 permutations (randomize fMRI of Brain Software Library program[29]), with the cluster-extent threshold option (whole-brain correction). Given the skewed ethnic/racial distribution of the sample across genotypes (Table 1), sensitivity analyses were conducted by rerunning the aforementioned analyses including exclusively Caucasian participants—the largest and most equally distributed group. Based on the VBM findings (see Section 3.2), the primary fixel-based WM morphometry analyses focused on the right and left CRUS I and CRUS II regions of interest (ROIs; Harvard-Oxford cortical and subcortical atlas[30]). However, exploratory analyses were also conducted in two additional ROIs: the right middle temporal gyrus and right anterior temporal fusiform cortex. These ROIs were selected for exploratory analyses because VBM analyses detected significant genotypic differences in at least 5% of the voxels of each ROI (right middle temporal gyrus: 28.3%, right anterior temporal fusiform cortex: 20.7%). In these masked WM analyses, only WM tracts originating from, or connecting

TABLE 1 Demographic characteristics across *FTO* genotype groups and comparing participants with and without MRI scans

Characteristic	CC (15)	CT (31)	TT (47)	Test statistic (*df*)	*p* value	Sample with usable MRI (93)	Sample without usable MRI (106)	Test statistic (*df*)	*p* value
Sex				$\chi^2_1 = 0.37$	0.83			$\chi^2_1 = 0.44$	0.51
Male	7	13	23			43	54		
Female	8	18	24			50	52		
Age	9.20 (1.26)	8.99 (1.16)	9.05 (1.15)	$F_{2,90} = 0.38$	0.68	9.03 (1.65)	7.89 (1.15)	$F_{1,197} = 34.30$	0.01
BMI	17.66 (2.62)	17.72 (3.40)	17.06 (2.08)	$F_{2,90} = 0.47$	0.63	17.37 (2.65)	17.40 (3.12)	$F_{2,197} = 0.001$	0.98
BMI Z-score	0.38 (0.91)	0.33 (1.08)	0.20 (0.78)	$F_{2,90} = 0.31$	0.74	0.27 (0.90)	0.38 (1.11)	$F_{2,197} = 0.59$	0.44
Race				$\chi^2_6 = 20.47$	0.01			$\chi^2_4 = 3.95$	0.41
Caucasian	13	12	10			35	38		
African American	0	5	15			21	34		
Asian	0	3	5			3	6		
Other	2	9	12			27	22		

to, the aforementioned ROIs were included. Fixel-based nonparametric statistical analyses were carried out with MRtrix. Correction for multiple comparisons was performed using the family-wise error (FWE) rate correction. Seed-based functional connectivity analyses were restricted to the aforementioned ROIs (from the Harvard-Oxford Atlas). Analyses included FD as a covariate and were thresholded at a voxel level $p < 0.001$ (uncorrected) and at a cluster level $p < 0.05$ (false discovery rate [FDR] corrected).

3 | RESULTS

3.1 | Demographics

Table 1 shows demographic data across groups and participants with and without usable MRI data. Age ($F_{2,90} = 0.38$, $p = 0.68$), sex ($\chi^2_1 = 0.37$, $p = 0.83$), BMI ($F_{2,90} = 0.47$, $p = 0.63$) and BMI Z-scores ($F_{2,90} = 0.31$, $p = 0.74$) did not differ across the homozygous allele carriers. Racial distributions differed between the groups, where the CC group was primarily composed of Caucasian participants and the CT and TT groups were more diverse ($\chi^2_6 = 20.47$, $p = 0.01$). Children with and without usable MRI scans differed in age ($F_{1,197} = 34.30$, $p = 0.01$), with the scanned sample being older, but did not differ in BMI ($F_{2,197} = 0.001$, $p = 0.98$), sex ($\chi^2_1 = 0.44$, $p = 0.51$) or race/-ethnicity ($\chi^2_4 = 3.95$, $p = 0.41$).

3.2 | GM volumes

Compared with the TT group, the CC group demonstrated significantly greater GM volume in a number of regions, primarily including the bilateral cerebellum, temporal gyrus, temporal fusiform cortex and brain stem ($_{peak}t$s = 4.81–1.30; ps = 0.017–0.050). Further, the CC group demonstrated volumetric increases in the right parahippocampal ($_{peak}t = 2.69$; $p = 0.021$) and occipital fusiform gyri ($_{peak}t = 1.38$; $p = 0.049$). Similar effects were noted comparing the CC and CT group. Specifically, the CC group showed larger volumes in the bilateral cerebellum and several regions in the medial and inferior temporal lobe ($_{peak}t$s = 4.74–2.27; ps = 0.036–0.042). There were no significant differences in GM volume between the CT and TT groups. See Figure 3 and Table 2 for details. All differences were significant at a whole-brain corrected p value <0.05 (randomization permutation; effect size and percentage volume difference maps shown in Figure 4).

Albeit not statistically significant due to reduced power ($N = 35$), sensitivity analyses demonstrated similar findings within Caucasian participants, with the CC group demonstrating greater GM volumes than the CC (ps = 0.076–0.236) and TT groups (ps = 0.132–0.250; Figure 5). Given prior MRI literature finding evidence for additive *FTO* effects,[5,6,12] additional analyses using linear regression models tested for dose-dependent effects but did not find any support ($p = 0.82$).

3.3 | WM connectivity

Because VBM findings suggested significant genotype-associated structural differences in the cerebellum, particularly in the Crus I and Crus II cerebellar subregions, primary WM analyses focused on the structural connectivity of these regions. In analyses of the right and left Crus I and Crus II connectivity, children in the CC group, relative to the TT group, demonstrated increased FDC in the middle cerebellar peduncle ($_{peak}t$s = 6.19–6.34; ps$_{FWE}$ = 0.037–0.042) and increased fibre-bundle cross section (FC) in the tract connecting the left corticospinal to middle cerebellar peduncle ($_{peak}t$s = 4.33–4.75; ps$_{FWE}$ = 0.004–0.005). Analyses examining the connectivity of the middle temporal gyri showed that children in the CC group

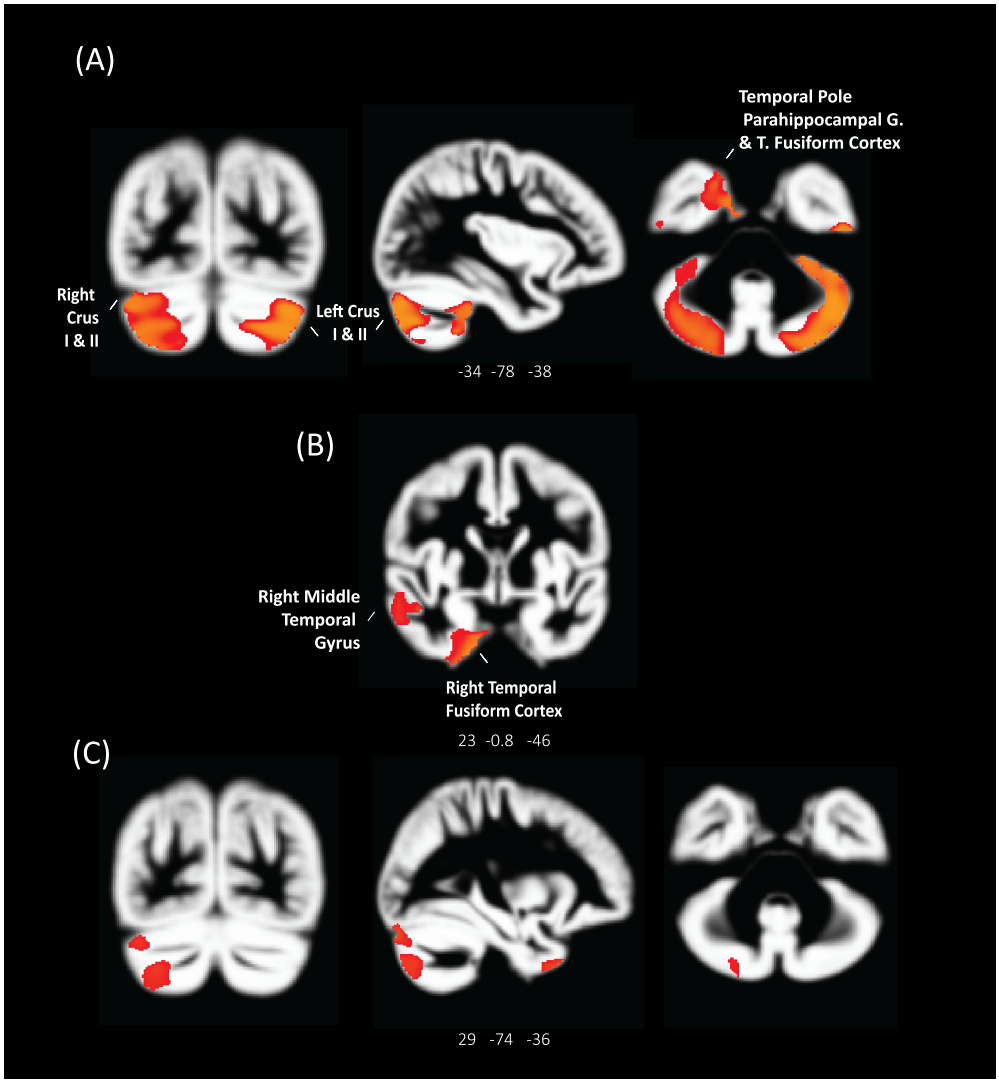

FIGURE 3 Differences in grey matter volumes (voxel-based morphometry) across *FTO* genotype groups. Significant group volume differences across *FTO* genotypes were detected. Analyses were conducted on grey matter (GM) volume maps, estimated from T1-weighted magnetic resonance imaging and through voxel-based morphometry, using a whole-brain corrected $p < 0.05$ (randomization permutation; cluster-extent based correction), controlling for age, sex and body mass index (BMI). Coloured areas show greater volumes in the CC versus TT groups. The CC group showed greater volume in a number of regions, including the bilateral cerebellum (A), as well as the middle temporal gyrus and temporal fusiform cortex (B). Differences were also detected when comparing the CC and CT groups with the CC group showing greater volumes in a number of regions, including the right cerebellum, middle temporal gyrus and temporal fusiform cortex (C). Analyses did not detect significant differences between CT and TT findings

demonstrate increased FC in the right uncinate fasciculus ($_{peak}t$ = 4.84; p_{FWE} = 0.019). Analyses of right anterior temporal fusiform connectivity showed that children in the CC group demonstrate increased FC and FDC in the right inferior longitudinal fasciculus ($_{peak}t$s = 4.55 and 5.02; ps_{FWE} = 0.031 and 0.037, respectively). In analyses of the right and left Crus I and Crus II connectivity, children in the CC group, relative to the CT group, demonstrated increased FC the tract connecting the bilateral corticospinal to middle cerebellar peduncle ($_{peak}t$s = 4.07–4.10; ps_{FWE} = 0.002–0.003) and increased FDC in the tract connecting the left and bilateral corticospinal to middle cerebellar peduncle ($_{peak}t$s = 4.79–5.10; ps_{FWE} = 0.036–0.039). CC children also demonstrated increased FC in the right inferior longitudinal fasciculus ($_{peak}t$ = 3.68; p_{FWE} = 0.040). No significant differences were detected between the CT and TT groups. See Figure 6 and Table 3 for details.

3.4 | Functional connectivity

Primary resting-state connectivity analyses focused on Crus I and Crus II, and these bilateral ROIs were used as seeds. Compared with the TT group, the CC group demonstrated increased positive connectivity (i.e., positive correlation) between the right Crus I and clusters in the right cerebellum (Crus II, VIII, and VIIb; t = 4.20; p_{fdr} = 0.002) and

TABLE 2 Grey matter volumes (voxel-based morphometry) across *FTO* genotype groups

Contrast	Regions	MNI coordinates x	y	z	Hemisphere	Cluster size	Whole-brain corrected *p* value
CC > TT	Temporal gyrus, temporal fusiform cortex, cerebellum (Crus I, Crus II, VI, VIIb, VIIa, and VIIIa)	87	64	38	L	5398	0.017
	Cerebellum (Crus I, Crus II, VI, VIIb, and VIIIa)	43	27	36	R	4248	0.018
	Brain stem, para-hippocampal gyrus, temporal fusiform cortex, and temporal gyrus	45	87	22	R	1689	0.021
	Temporal pole, middle and superior temporal gyrus (anterior)	31	86	32	R	928	0.026
	Middle temporal gyrus	15	65	44	R	132	0.046
	Brain stem and cerebellum (X)	49	59	24	R	17	0.049
	Occipital fusiform gyrus and lateral occipital cortex	35	40	39	R	11	0.049
	Middle temporal gyrus	17	65	39	R	10	0.050
CC > CT	Cerebellum (Crus II, Crus I, and Crus VIIB)	41	33	24	R	774	0.040
	Cerebellum (Crus 1 and Crus II)	42	27	35	R	538	0.036
	Cerebellum (V, I V, I-IV, and Vermis IV)	61	40	40	L	314	0.039
	Temporal pole, inferior temporal gyrus, and temporal fusiform cortex	44	93	24	R	273	0.036
	Temporal pole, middle temporal gyrus	31	87	32	R	90	0.042

Note: R, right; L, left.

regions in the right frontal gyrus (t = 4.10; p_{fdr} = 0.011). Differences also emerged in left Crus I connectivity, where CC children showed increases in connectivity to the right planum polare (t = 3.98; p_{fdr} = 0.032). CC children also demonstrated increased positive connectivity between left Crus II and the right superior temporal gyrus (t = 5.10; p_{fdr} < 0.001), as well as clusters covering regions of the right putamen, pallidum, and amygdala (t = 4.38; p_{fdr} < 0.001), and the left temporal (t = 4.22; p_{fdr} = 0.019) and superior frontal gyrus (t = 3.68; p_{fdr} = 0.039). Exploratory analyses using the right anterior temporal fusiform cortex as a seed suggested that compared with TT allele carriers, children in the CC group showed increased connectivity with a cluster covering regions of the right temporal occipital fusiform cortex and cerebellum VI (t = 4.60; p_{fdr} = 0.023). Analyses examining right middle temporal gyrus connectivity did not yield significant results. Compared with CT carriers, CC allele carriers showed increased negative connectivity from the left Crus I to the brain stem (t = 4.25; p_{fdr} = 0.017). Further, CT allele carriers demonstrated increased connectivity from the right Crus I to the right temporal occipital fusiform cortex (t = 4.82; p_{fdr} < 0.001) and other right cerebellar regions (t = 4.73; p_{fdr} = 0.003), as compared with children in the TT group. Refer to Figure 7 and Table 4. Figure 8 shows connectivity patterns across groups.

4 | DISCUSSION

This is the first study to examine brain structure and function in relationship to *FTO* SNP rs1421085 obesity-risk alleles in young children without obesity. It is thus the first study to identify *FTO*-associated differences in brain structure and architecture before the onset of obesity, which would confound the ability to observe the primary genotypic effect. Multimodal analyses identified genotype-associated alterations in bilateral cerebellar GM, WM and functional connectivity, as well alterations in the right middle gyrus and fusiform cortex. Specifically, homozygous risk allele carriers (CC) show increased bilateral cerebellar and right fusiform cortex volume, as well as increased cerebellar structural and functional connectivity, compared with homozygous nonrisk allele carriers (TT).

Existing adult *FTO* neuroimaging studies have primarily focused on examining impulse control and reward processing neurocircuitry. To date, a handful of studies align with the present findings and document differences in cerebellar structure and functioning. In one study,[14] temperamental sensitivity towards reward was positively related to cerebellum resting state connectivity in rs9939609 *FTO* risk allele carriers. Homozygous nonrisk allele carriers showed negative correlations between cerebellar connectivity and this temperamental profile.[14] The authors interpreted these findings as suggestive of risk allele carriers attributing a greater reward value to food. Similarly, Wiemerslage and colleagues reported that homozygous risk allele carriers showed differences in cerebellar activation when viewing images of high versus low calorie foods, whereas homozygous rs9939609 nonrisk allele carriers did not.[9] Within risk allele carriers, the direction of the findings differed depending on participants' BMI: participants with higher BMI showed decreased activation to high-calorie foods, whereas the opposite was true for participants with lower BMI. The authors suggest that these findings reflect differences in the neural processing of food caloric discrimination, with only risk allele carriers showing cerebellar activation in this process. Conversely, Melhorn

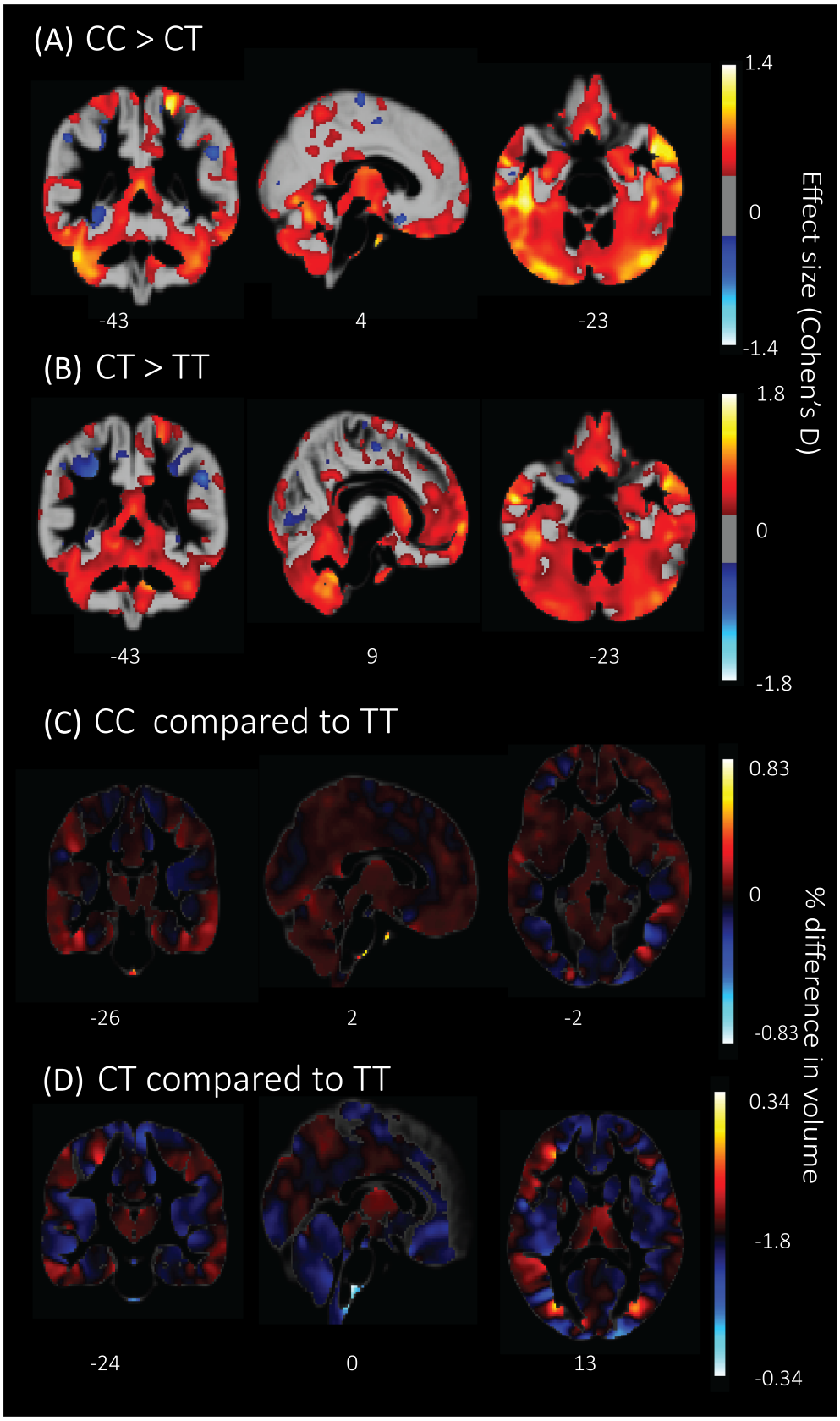

FIGURE 4 Effect size and percentage volume difference maps for the grey matter volumetric differences across *FTO* genotype groups. Cohen's *d* maps demonstrate effect size estimates from the grey matter volumetric analyses across *FTO* genotype groups (A,B). Percentage differences in volumes between the different carrier groups were also calculated (C,D). The homozygous low risk allele carrier group (TT) was used as a reference group. Percentage volume differences were computed for each voxel

and colleagues[10] described an association between food images and cerebellar activity in the "lower risk group" (rs9939609 AA/TT vs. AA), where nonfattening foods elicited more activity than nonfood objects. Finally, one adult structural study also documented Crus I volumetric alterations, yet risk allele carriers demonstrated increased volume in this region (used a tagging SNP for rs1421085 and rs17817449).[4]

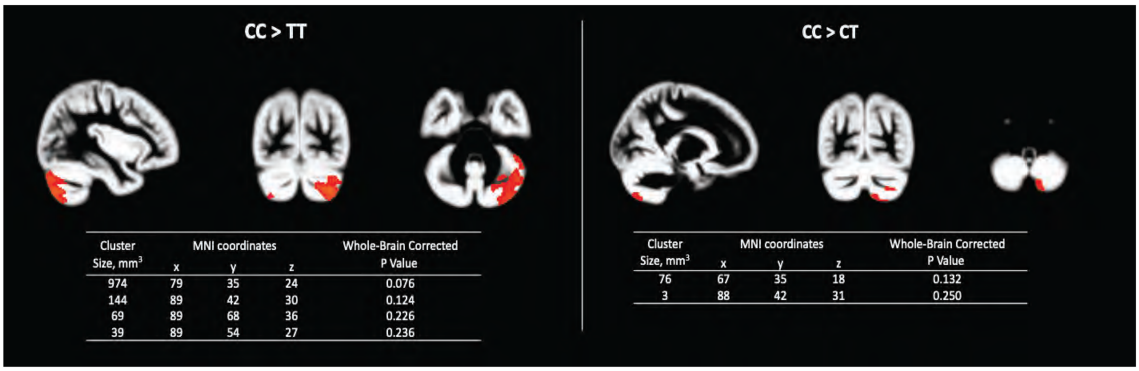

Cluster Size, mm³	MNI coordinates x	y	z	Whole-Brain Corrected P Value
974	79	35	24	0.076
144	89	42	30	0.124
69	89	68	36	0.226
39	89	54	27	0.236

Cluster Size, mm³	MNI coordinates x	y	z	Whole-Brain Corrected P Value
76	67	35	18	0.132
3	88	42	31	0.250

FIGURE 5 Sensitivity analysis: grey matter volumes across *FTO* genotype groups within Caucasian participants only. Sensitivity analysis of explored grey matter volumes across *FTO* genotype groups within the Caucasian participants only. This was the largest racial/ethnic group included in the study and the one most equally distributed across genotypes

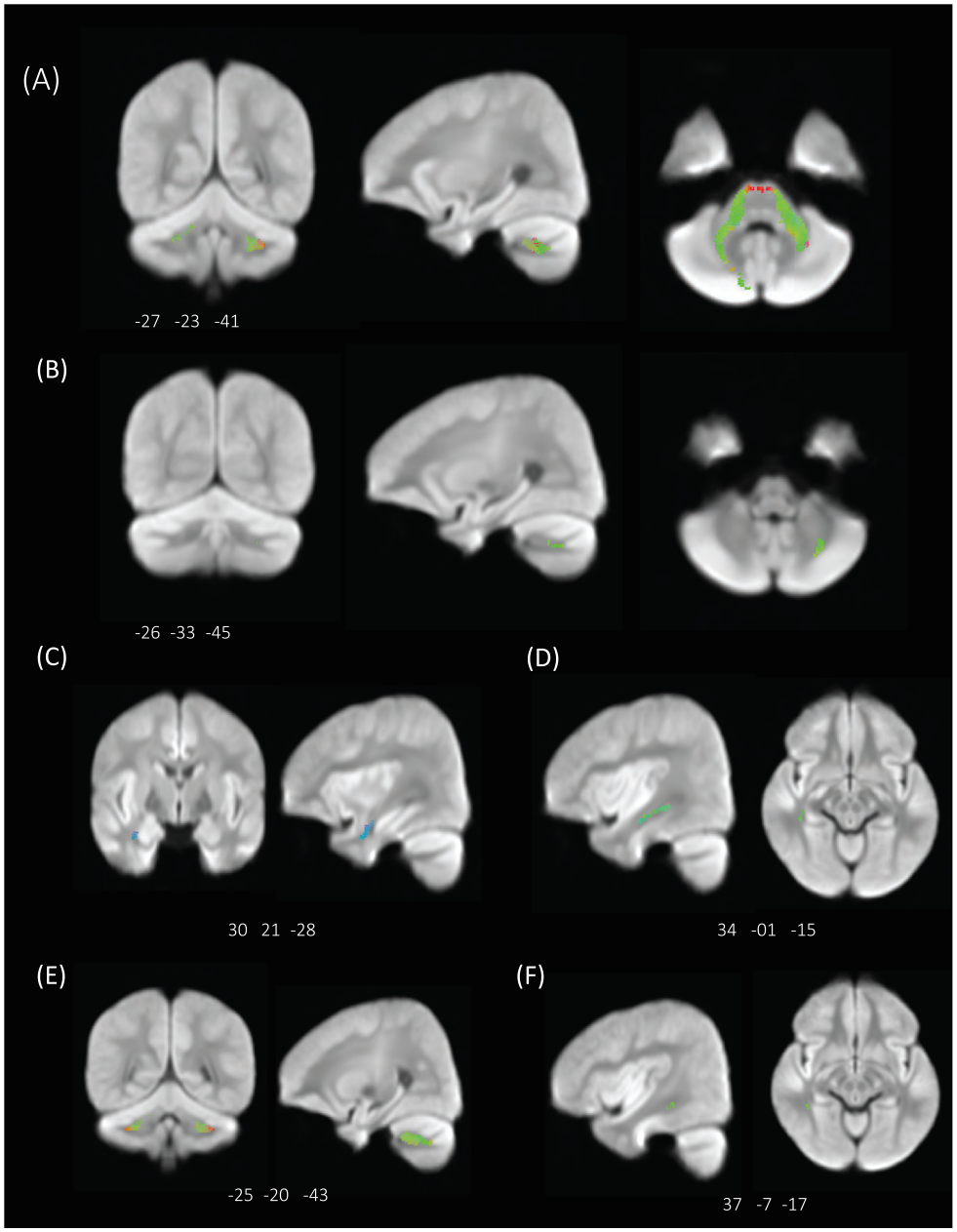

FIGURE 6 Differences in white matter connectivity (fixel-based morphometry) related to *FTO* genotype. Primary fixel-based white matter (WM) morphometry analyses restricted to the right and left CRUS I and CRUS II regions of interest (ROIs) showed increased fibre density and cross section (FDC) and fibre-bundle cross section (FC) between the CC and TT groups; $p_{FWE} < 0.05$; coloured areas mark FDC and FC differences. In analyses of the left Crus II (A), children in the CC group demonstrated increased FDC in the middle cerebellar peduncle (A) and increased FC (B) in the tract connecting the left corticospinal to middle cerebellar peduncle. CC children also demonstrated increased right FC in the uncinate fasciculus (C) and FC and FDC in the right inferior longitudinal fasciculus (D). Analyses focused on the right Crus I showed that, compared with the CT group, CC children had higher FC in the bilateral corticospinal tract to the middle cerebellar peduncle (E). CC children also demonstrated increased FC in the right inferior longitudinal fasciculus (F). No significant differences were detected between the CT and TT groups. Significant streamlines are coloured by direction (anterior–posterior: green; superior–inferior: blue; left–right: red)

TABLE 3 White matter connectivity (fixel-based morphometry) across *FTO* genotype groups

Seed	Contrast	Measure	Region	Cluster size	Peak *t* value	Peak *p* value
Right Crus I	CC > TT	FDC	Middle cerebellar peduncle	6	6.19	0.042
		FC	Left corticospinal tract to middle cerebellar peduncle	1954	4.33	0.005
	CC > CT	FDC	Left corticospinal tract to middle cerebellar peduncle	21	4.79	0.038
		FC	Bilateral corticospinal tract to middle cerebellar peduncle	2430	4.08	0.003
Left Crus I	CC > TT	FDC	Middle cerebellar peduncle	22	6.32	0.039
		FC	Left corticospinal tract to middle cerebellar peduncle	1836	4.75	0.005
	CC > CT	FDC	Left corticospinal tract to middle cerebellar peduncle	36	4.79	0.038
		FC	Bilateral corticospinal tract to middle cerebellar peduncle	2475	4.09	0.002
Right Crus II	CC > TT	FDC	Middle cerebellar peduncle	8	6.32	0.042
		FC	Left corticospinal tract to middle cerebellar peduncle	1999	4.74	0.004
	CC > CT	FDC	Left corticospinal tract to middle cerebellar peduncle	18	4.80	0.039
		FC	Bilateral corticospinal tract to middle cerebellar peduncle	2404	4.10	0.003
Left Crus II	CC > TT	FDC	Middle cerebellar peduncle	23	6.34	0.037
		FC	Left corticospinal tract to middle cerebellar peduncle	1886	4.75	0.005
	CC > CT	FDC	Bilateral corticospinal tract to middle cerebellar peduncle	31	5.10	0.036
		FC	Bilateral corticospinal tract to middle cerebellar peduncle	2497	4.07	0.003
Anterior middle temporal gyrus	CC > TT	FC	Right uncinate fasciculus	152	4.84	0.019
	CC > CT	FC	Right inferior longitudinal fasciculus	28	3.68	0.040
Right temporal fusiform cortex	CC > TT	FC	Right inferior longitudinal fasciculus	47	4.55	0.031
		FDC	Right inferior longitudinal fasciculus	15	5.02	0.037

Note: All fixels are significant at family-wise error (FWE) $p < 0.05$.
Abbreviations: FD, fibre density; FDC, fibre density and cross section.

The four above-mentioned studies suggest that cerebellar structure and function differs as a function of *FTO* genotype and may somehow be related to food salience and reward evaluation. However, the studies all differ in a number of critical features that make identifying the specific source of variability a considerable challenge. Melhorn, Kühn, and Wiemerslage all examine brain activity to food image viewing, yet Kühn only examines cerebellar structure, and not activity. Melhorn utilizes a twin sample, Wiemerslage's sample is composed of males, and none of the studies define their genotype groups similarly (Kühn uses the recessive model, Melhorn the dominant model, and Wiemerslage compares homozygous allele carriers). Further, Wiemerslage's sample shows significant BMI differences and includes overweight participants, whereas Melhorn uses a matched sample of participants with average BMI. Thus, although the present findings are consistent with some of the existing literature, the use of mixed methodologies and exclusion of the cerebellum from analyses in nearly half of the existing literature[7,11,12] precludes studies from ascertaining what role, if any, the cerebellum plays in *FTO*-related risk for obesity. Of note, the four aforementioned studies documenting *FTO* differences all examined different *FTO* SNPs (rs1421085, rs17817449, and rs9939609). Given that these SNPs are in strong (pairwise $r^2 > 0.97$),[31] but not perfect, linkage disequilibrium, extrapolating findings from one study to another should be done with caution.

Nevertheless, the cerebellum is increasingly gaining recognition as being involved in higher order functions, including reward-based learning, attention, emotion and executive functions.[32,33] Discovery of reciprocal cerebellar-hypothalamic connections has led to the

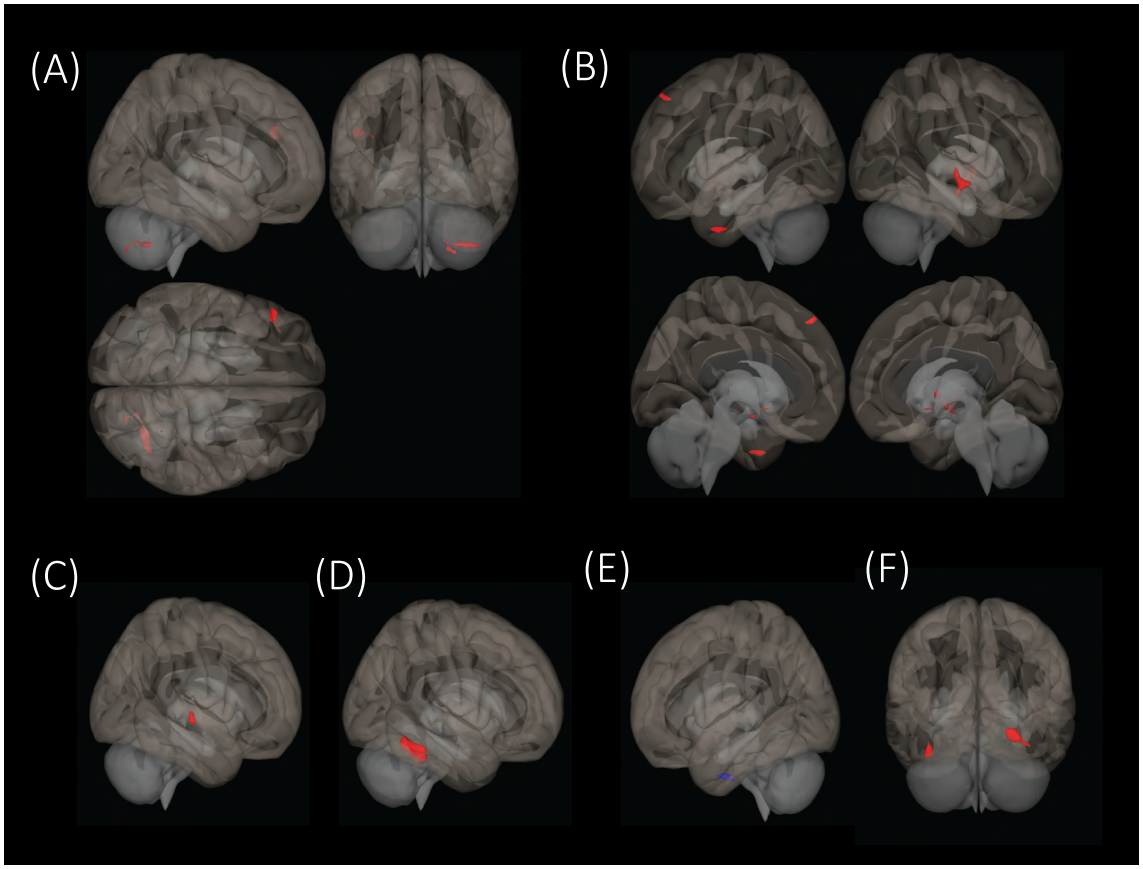

FIGURE 7 Differences in resting state functional connectivity related to *FTO* genotype. Using the bilateral Crus I and Crus II regions as seeds, seed-based functional connectivity contrasts detected a number of differences between homozygous allele carriers. Analyses were thresholded at a voxel level $p < 0.001$ (uncorrected) and at a cluster level $p < 0.05$ (false discovery rate [FDR] corrected). Coloured areas show increases in positive (red) connectivity between the groups. Compared with the TT group, the CC group demonstrated increased positive connectivity between the right Crus I (A) and clusters in the right cerebellum (Crus II, VIII and VIIb) and regions in the right frontal gyrus. CC children also demonstrated increased positive connectivity between left Crus I (B) and II (C) and a number of regions, including the right putamen, pallidum and left temporal and superior frontal gyrus. Exploratory analyses of anterior temporal fusiform cortex connectivity found that children in the CC group showed increased connectivity with the right temporal occipital fusiform cortex and cerebellum VI (D). (E) and (F) show functional connectivity contrasts comparing CC versus CT and CT versus TT allele carriers

hypothesis that the cerebellum may have a role in the regulation of eating behaviours.[34,35] Leptin receptors are densely expressed in the cerebellum and involved in cerebellar responsivity to food-cues.[36] Further, *FTO* is widely expressed in the cerebellum.[37] A substantial body of literature has reported differences in brain structure and function associated with BMI. Studies in adults have found negative associations between BMI and cerebellum GM volume[38,39] (but see Bauer et al[40]). Lower cerebellar GM volume has been related to increased waist circumference,[41,42] fat mass index[43] and intra-abdominal adiposity.[44] Surprisingly, one study found reductions in cerebellar GM volume post caloric restriction-induced weight loss.[45] BMI-associated differences in cerebellum WM connectivity have also been reported (WM expansion[46] and decreased fractional anisotropy[47]), yet the direction of findings has differed, possibly due to the different measures employed. Obesity per se may influence cerebellar function. For example, studies suggest functional differences at rest (increased salience network connectivity correlated with BMI,[48] reduced eigenvector centrality in participants with higher visceral adipose tissue[44] and increased negative cerebellum–ventral striatum connectivity in participants with obesity[49]), postmeal (greater decreases in regional blood flow in men with obesity[50]), when viewing food images,[51] and after weight loss (reduced hypothalamus–cerebellum connectivity[52]). Of note, one study described that participants with higher BMI had increased cerebellum activity in response to gastric distension by balloon inflation, compared with participants with average BMI, suggesting that the cerebellum could play a role in mediating meal-related aspects of ingestive behaviours.[53]

Analyses also detected significant volumetric increases in the temporal fusiform cortex and middle temporal gyrus, as well as increased structural and functional fusiform connectivity. Notably, these findings overlap with a prior adult study where FTO risk allele carriers showed increased fusiform activity when viewing food images,[4] as well as volumetric alterations in fusiform gyrus volume (which predicted allele group membership [AA/AT vs. TT] with 91%

TABLE 4 Functional connectivity by *FTO* genotype groups and across all participants

Contrast	Seed	Region	MNI coordinates x	y	z	Direction	Hemisphere	Number of voxels	Size *p*-FDR	Peak *t* value	Peak Z value
CC > TT	Crus I—R	Cerebellum (Crus II, VIII, and VIIb)	22	−76	−50	+	R	167	0.001852	4.20	2.94
		Middle frontal gyrus	−48	32	28	+	L	110	0.011153	4.10	3.85
	Crus I—L	Planum polare and Heschl's gyrus	46	−18	0	+	R	86	0.032044	3.98	3.75
	Crus II—L	Planum polare, middle and superior temporal gyrus	44	−16	2	+	R	222	0.000055	5.10	4.67
		Putamen, pallidum, and amygdala	12	−2	0	+	R	150	0.000607	4.38	4.09
		Inferior temporal gyrus	−58	−2	−38	+	L	75	0.018828	4.22	3.95
		Subcallosal cortex	−4	−6	−14	+		65	0.025597	4.08	3.84
		Superior frontal gyrus	−4	42	50	+	L	55	0.038307	3.68	3.49
	Right temporal fusiform cortex	Temporal occipital fusiform cortex and Cerebellum VI	32	−40	−26		R	421	0.023488	4.60	4.27
CC > CT	Crus I—L	Brain stem	−8	−8	−36	–		85	0.017400	4.25	3.98
CT > TT	Crus I—R	Occipital fusiform and lingual gyrus	24	−62	−8	+	R	200	0.000125	4.82	4.46
		Temporal occipital fusiform cortex and cerebellum (Crus I and VI)	−34	−60	−22	+	L	109	0.002923	4.73	4.39
Across all participants	Crus I—R	Cerebellum (Crus I and VI)	38	−64	−28	+	R	160	0.000817	4.46	4.16
		Posterior cingulate gyrus	−6	−46	32	+	L	82	0.014269	4.22	3.96
	Crus I—L	Frontal pole	0	66	10	+	R/L	64	0.049429	4.39	4.10
		Inferior posterior temporal gyrus	52	−18	−32	+	R	58	0.049429	3.91	3.70
	Crus II—R	Precuneus, posterior cingulate gyrus	0	−54	34	+	R	173	0.000279	5.10	4.86
		Cerebellum (Crus I, II, and IIb)	48	−56	−50	+	R	155	0.000303	4.37	4.09
		Brains stem	−4	−30	−38	+		56	0.030460	4.27	4.00
	Crus II—L	Middle and superior frontal gyrus	24	32	38	+	R	227	0.000034	5.28	4.82
		Cerebellum (II, VII, and I)	−32	−62	−40	+	L	214	0.000034	4.80	4.44
		Precuneus	38	−58	22	+	R	97	0.004849	4.62	4.29
		Temporal pole	48	2	−24	+	R	90	0.005299	4.19	3.94
		Middle frontal gyrus	−36	20	46	+	L	56	0.031108	3.82	3.62
		Hippocampus	14	−18	−16	–	R	86	0.035993	4.89	4.51
	Anterior middle temporal gyrus	Posterior middle temporal gyrus and superior anterior temporal gyrus	56	−12	−22	+	R	527	0.006706	6.33	5.59

Note: R, right; L, left; +, positive connectivity; –, negative connectivity.
Abbreviation: FDR, false discovery rate.

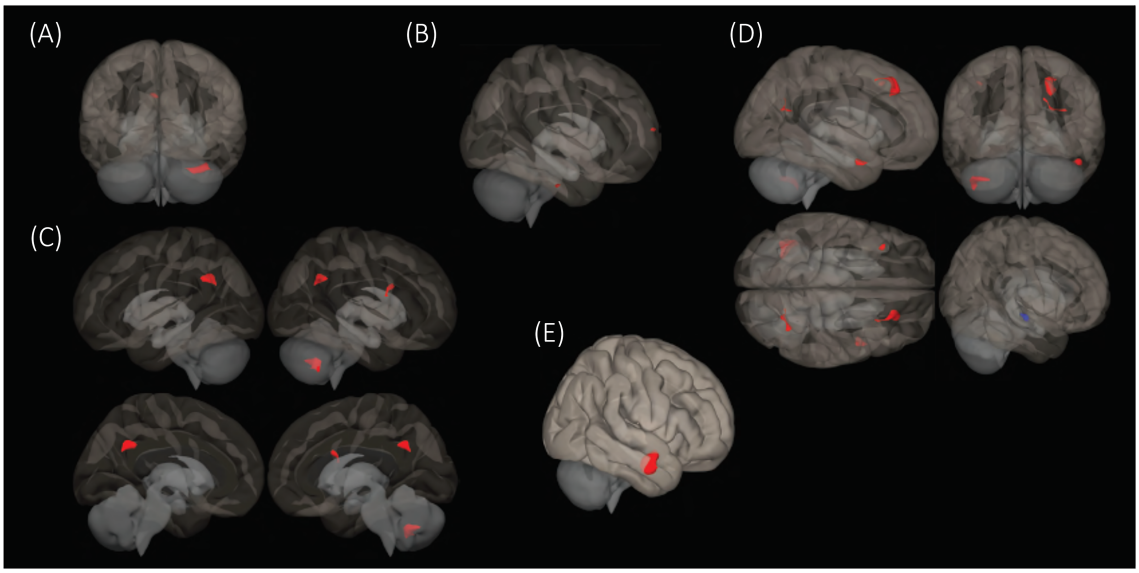

FIGURE 8 Resting state functional connectivity patterns across all participants. Across groups, seed-based connectivity maps generated from the right Crus I (A) and II (C) showed significant positive connectivity to the posterior cingulate gyrus, precuneus and other right cerebral regions. Analyses of the left Crus I (B) and II (D) showed positive connectivity to several regions within the frontal cortex, temporal gyrus and right frontal pole. The left Crus II also demonstrated significant negative connectivity to the right hippocampus. Exploratory analyses of anterior middle temporal fusiform connectivity showed significant positive connectivity to the posterior division of the of the middle temporal fusiform connectivity (E). Coloured areas show increases in positive (red) and negative (blue) connectivity between the groups. Analyses were thresholded at a voxel level $p < 0.001$ (uncorrected) and at a cluster level $p < 0.05$ (false discovery rate [FDR] corrected)

accuracy). A further adult study documented that the relationship between fusiform cortex reactivity to viewing food images and circulating acyl-ghrelin levels varied as a function of *FTO* genotype.[13] Because *FTO* regulates ghrelin, an important mediator of ingestive behaviours, these findings were interpreted as suggestive of the fusiform cortex having a homeostatic role in said behaviours. Further, a number of studies find increased fusiform cortex activation in hungry versus satiated participants.[54] Together, these studies suggest that the fusiform gyrus might extend beyond face perception and have a role in the processing and valuation of food stimuli and that this mechanism might be particularly important in trying to understand the neural underpinnings of *FTO*.[10]

However, findings must be interpreted with caution due to important study limitations. Results must be replicated in larger samples with more symmetrical group sizes, enabling the examination of possible *FTO* genotype interactions with other participant level characteristics, such as sex and ethnicity. This caveat is particularly true for resting state analyses, in which many participants had to be excluded due to motion, and analyses may be particularly underpowered. Further, the functional significance of the brain differences detected can only be determined by a longitudinal examination of the relationship between cerebellar differences and food intake and other eating-related behaviours. Given prior reports of interactions between *FTO* genotype and temperament in predicting brain activity,[14] studies should also include assessments of child temperament, particularly reward sensitivity and inhibitory control. In order to disambiguate effects on the cerebellum of *FTO* risk allele from those of BMI per se, weight gain and diet,[15,55] future studies should use repeated measures prospective study designs to examine cerebellar structure and function, recruiting children prior to the onset of obesity and following them over time as weight gain progresses.

In sum, the study findings add to the accumulating body of literature suggesting differences in cerebellar structure and function are related to *FTO* genotype. These differences may be associated with aspects of ingestive behaviours, yet little attention had been placed on thoroughly understanding the cerebellum's role in any of these factors. Purposefully examining cerebellar structure and function in relation to eating behaviours and obesity could elucidate important aspects of the neural substrates of this major public health concern.

FUNDING INFORMATION

NIDDK grants R56/R01 DK097399, R01-DK52431 and 5P30DK026687 and National Institutes of Health Clinical and Translational Science Award (CTSA), awarded by The Irving Institute for Clinical and Translational Science, Columbia University, New York, NY UL1 TR000040

ACKNOWLEDGEMENTS

The authors acknowledge the contribution of all of the dedicated staff who participated in this study and recognize Patricia Lanzano and Liyong Deng for their technical support. We thank all the families who participated in this study.

CONFLICT OF INTEREST

The authors declared no conflict of interest.

ORCID

Claudia Lugo-Candelas https://orcid.org/0000-0002-8388-9479
Lisa Ranzenhofer https://orcid.org/0000-0002-7199-6998
Michael Rosenbaum https://orcid.org/0000-0003-2835-9202

REFERENCES

1. Frayling TM, Timpson NJ, Weedon MN, et al. A common variant in the *FTO* gene is associated with body mass index and predisposes to childhood and adult obesity. *Science*. 2007;316:889-894. https://doi.org/10.1126/science.1141634
2. Ranzenhofer LM, Mayer LES, Davis HA, Mielke-Maday HK, McInerney H, Korn R, Gupta N, Brown AJ, Schebendach J, Tanofsky-Kraff M, Thaker V, Chung WK, Leibel RL, Walsh BT, Rosenbaum M The FTO gene and measured food intake in 5- to 10-year-old children without obesity. *Obesity (Silver Spring, Md)*. 2019;27(6):1023–1029. Epub 2019/05/24. https://doi.org/10.1002/oby.22464. PubMed PMID: 31119882; PubMed Central PMCID: PMCPMC6561098.
3. Berentzen T, Kring SI, Holst C, Zimmermann E, Jess T, Hansen T, Pedersen O, Toubro S, Astrup A, Sørensen TI Lack of association of fatness-related FTO gene variants with energy expenditure or physical activity. *J Clin Endocrinol Metab* 2008;93(7):2904–2908. Epub 2008/05/01. https://doi.org/10.1210/jc.2008-0007. PubMed PMID: 18445669.
4. Kühn AB, Feis D-L, Schilbach L, et al. FTO gene variant modulates the neural correlates of visual food perception. *NeuroImage*. 2016;128:21-31. https://doi.org/10.1016/j.neuroimage.2015.12.049
5. Ho AJ, Stein JL, Hua X, et al. A commonly carried allele of the obesity-related *FTO* gene is associated with reduced brain volume in the healthy elderly. *Proc Natl Acad Sci U S a*. 2010;107:8404-8409.
6. de Groot C, Felius A, Trompet S, et al. Association of the fat mass and obesity-associated gene risk allele, rs9939609A, and reward-related brain structures. *Obesity*. 2015;23:2118-2122. https://doi.org/10.1002/oby.21191
7. Olivo G, Latini F, Wiemerslage L, Larsson E-M, Schiöth HB. Disruption of accumbens and thalamic white matter connectivity revealed by diffusion tensor tractography in young men with genetic risk for obesity. *Frontiers in Human Neuroscience*. 2018;12. https://doi.org/10.3389/fnhum.2018.00075
8. Dennis EL, Jahanshad N, Braskie MN, Warstadt NM, Hibar DP, Kohannim O, Nir TM, McMahon KL, de Zubicaray GI, Montgomery GW, Martin NG, Toga AW, Wright MJ, Thompson PM Obesity gene NEGR1 associated with white matter integrity in healthy young adults. *NeuroImage*. 2014;102(2):548–557. https://doi.org/10.1016/j.neuroimage.2014.07.041. PubMed PMID: PMC4269485.
9. Wiemerslage L, Nilsson EK, Solstrand Dahlberg L, Ence-Eriksson F, Castillo S, Larsen AL, Bylund SB, Hogenkamp PS, Olivo G, Bandstein M, Titova OE, Larsson EM, Benedict C, Brooks SJ, Schiöth HB An obesity-associated risk allele within the FTO gene affects human brain activity for areas important for emotion, impulse control and reward in response to food images. *Eur J Neurosci* 2016;43(9):1173–1180. Epub 2016/01/23. https://doi.org/10.1111/ejn.13177. PubMed PMID: 26797854.
10. Melhorn SJ, Askren MK, Chung WK, et al. FTO genotype impacts food intake and corticolimbic activation. *Am J Clin Nutr*. 2018;107:145-154. https://doi.org/10.1093/ajcn/nqx029
11. Sevgi M, Rigoux L, Kuhn AB, Mauer J, Schilbach L, Hess ME, Gruendler TOJ, Ullsperger M, Stephan KE, Bruning JC, Tittgemeyer M An obesity-predisposing variant of the FTO gene regulates D2R-dependent reward learning. *The Journal of Neuroscience: The Official Journal of the Society for Neuroscience*. 2015;35(36):12584–12592. Epub 2015/09/12. https://doi.org/10.1523/jneurosci.1589-15.2015. PubMed PMID: 26354923.
12. Heni M, Kullmann S, Veit R, Ketterer C, Frank S, Machicao F, Staiger H, Häring HU, Preissl H, Fritsche A Variation in the obesity risk gene FTO determines the postprandial cerebral processing of food stimuli in the prefrontal cortex. *Molecular Metabolism*. 2014;3(2):109–113. https://doi.org/10.1016/j.molmet.2013.11.009. PubMed PMID: PMC3953703.
13. Karra E, O'Daly OG, Choudhury AI, et al. A link between FTO, ghrelin, and impaired brain food-cue responsivity. *J Clin Invest*. 2013;123:3539-3551. https://doi.org/10.1172/JCI44403
14. Olivo G, Wiemerslage L, Nilsson EK, Solstrand Dahlberg L, Larsen AL, Olaya Búcaro M, Gustafsson VP, Titova OE, Bandstein M, Larsson EM, Benedict C, Brooks SJ, Schiöth HB Resting-state brain and the FTO obesity risk allele: default mode, sensorimotor, and salience network connectivity underlying different somatosensory integration and reward processing between genotypes. *Frontiers in Human Neuroscience*. 2016;10:1-21. https://doi.org/10.3389/fnhum.2016.00052. PubMed PMID: PMC4756146.
15. Stice E, Yokum S, Blum K, Bohon C. Weight gain is associated with reduced striatal response to palatable food. *The Journal of neuroscience: the official journal of the Society for Neuroscience*. 2010;30(39):13105–13109. Epub 2010/10/01. doi: https://doi.org/10.1523/jneurosci.2105-10.2010. PubMed PMID: 20881128; PubMed Central PMCID: PMCPMC2967483.
16. Rapuano KM, Zieselman AL, Kelley WM, Sargent JD, Heatherton TF, Gilbert-Diamond D. Genetic risk for obesity predicts nucleus accumbens size and responsivity to real-world food cues. *Proc Natl Acad Sci*. 2017;114:160-165.
17. Gill R, Stratigopoulos G, Lee JH, Leibel RL. Functional genomic characterization of the FTO locus in African Americans. *Physiol Genomics* 2019;51(11):517–528. https://doi.org/10.1152/physiolgenomics.00057.2019. PubMed PMID: 31530225.
18. Cauchi S, Stutzmann F, Cavalcanti-Proenca C, Durand E, Pouta A, Hartikainen AL, Marre, M., Vol, S., Tammelin, T., Laitinen, J. and Gonzalez-Izquierdo, A. Combined effects of MC4R and FTO common genetic variants on obesity in European general populations. *Journal of molecular medicine (Berlin, Germany)*. 2009;87(5):537–546. Epub 2009/03/04. https://doi.org/10.1007/s00109-009-0451-6. PubMed PMID: 19255736.
19. Hudek A, Skara L, Smolkovic B, Kazazic S, Ravlic S, Nanic L, Osvatić, M.M., Jelčić, J., Rubelj, I. and Bačun-Družina, V. Higher prevalence of FTO gene risk genotypes AA rs9939609, CC rs1421085, and GG rs17817449 and saliva containing *Staphylococcus aureus* in obese women in Croatia. *Nutrition research (New York, NY)*. 2018;50:94–103. Epub 2018/03/16. https://doi.org/10.1016/j.nutres.2017.12.005. PubMed PMID: 29540276.
20. Sled JG, Zijdenbos AP, Evans AC. A nonparametric method for automatic correction of intensity nonuniformity in MRI data. *IEEE Trans Med Imaging*. 1998;17:87-97.
21. Smith SM. *BET: Brain Extraction Tool. FMRIB TR00SMS2b, Oxford Centre for Functional Magnetic Resonance Imaging of the Brain*. Headington, UK: Department of Clinical Neurology, Oxford University, John Radcliffe Hospital; 2000.
22. Kurth F, Gaser C, Luders E. A 12-step user guide for analyzing voxel-wise gray matter asymmetries in statistical parametric mapping (SPM). *Nat Protoc*. 2015;10:293-304. https://doi.org/10.1038/nprot.2015.014 https://www.nature.com/articles/nprot.2015.014#supplementary-information
23. Raffelt DA, Tournier JD, Smith RE, et al. Investigating white matter fibre density and morphology using fixel-based analysis. *NeuroImage*. 2017;144:58-73. https://doi.org/10.1016/j.neuroimage.2016.09.029

24. Raffelt DA, Smith RE, Ridgway GR, Tournier JD, Vaughan DN, Rose S, et al. Connectivity-based fixel enhancement: whole-brain statistical analysis of diffusion MRI measures in the presence of crossing fibres. *Neuroimage*. 2015;117:40–55. Epub 2015/05/26. https://doi.org/10.1016/j.neuroimage.2015.05.039. PubMed PMID: 26004503; PubMed Central PMCID: PMCPMC4528070.
25. Pruim RHR, Mennes M, van Rooij D, Llera A, Buitelaar JK, Beckmann CF. ICA-AROMA: a robust ICA-based strategy for removing motion artifacts from fMRI data. *Neuroimage* 2015;112:267–277. Epub 2015/03/17. https://doi.org/10.1016/j.neuroimage.2015.02.064. PubMed PMID: 25770991.
26. Power JD, Mitra A, Laumann TO, Snyder AZ, Schlaggar BL, Petersen SE. Methods to detect, characterize, and remove motion artifact in resting state fMRI. *NeuroImage*. 2014;84:320-341https://doi.org/10.1016/j.neuroimage.2013.08.048. https://doi/10.1016/j.neuroimage.2013.08.048. PubMed PMID: PMC3849338.
27. Whitfield-Gabrieli S, Nieto-Castanon A. Conn: a functional connectivity toolbox for correlated and anticorrelated brain networks. *Brain Connect* 2012;2(3):125–141. Epub 2012/05/31. https://doi.org/10.1089/brain.2012.0073. PubMed PMID: 22642651.
28. Cole JH, Boyle CP, Simmons A, et al. Body mass index, but not FTO genotype or major depressive disorder, influences brain structure. *Neuroscience*. 2013;252:109-117. https://doi.org/10.1016/j.neuroscience.2013.07.015
29. Winkler AM, Ridgway GR, Webster MA, Smith SM, Nichols TE. Permutation inference for the general linear model. *NeuroImage*. 2014;92:381-397. https://doi.org/10.1016/j.neuroimage.2014.01.060
30. Desikan RS, Segonne F, Fischl B, Quinn BT, Dickerson BC, Blacker D, Buckner, R.L., Dale, A.M., Maguire, R.P., Hyman, B.T. and Albert, M.S. An automated labeling system for subdividing the human cerebral cortex on MRI scans into gyral based regions of interest. *Neuroimage* 2006;31(3):968–980. Epub 2006/03/15. https://doi.org/10.1016/j.neuroimage.2006.01.021. PubMed PMID: 16530430.
31. Price RA, Li W-D, Zhao H. FTO gene SNPs associated with extreme obesity in cases, controls and extremely discordant sister pairs. *BMC Med Genet*. 2008;9:4-. doi: https://doi.org/10.1186/1471-2350-9-4. PubMed PMID: 18218107.
32. Adamaszek M, D'Agata F, Ferrucci R, Habas C, Keulen S, Kirkby KC, Leggio, M., Mariën, P., Molinari, M., Moulton, E. and Orsi, L. Consensus paper: cerebellum and emotion. *Cerebellum (London, England)*. 2017;16(2):552–576. Epub 2016/08/04. https://doi.org/10.1007/s12311-016-0815-8. PubMed PMID: 27485952.
33. Thoma P, Bellebaum C, Koch B, Schwarz M, Daum I. The cerebellum is involved in reward-based reversal learning. *Cerebellum (London, England)*. 2008;7(3):433–443. Epub 2008/07/02. https://doi.org/10.1007/s12311-008-0046-8. PubMed PMID: 18592331.
34. Zhu J-N, Wang J-J. The cerebellum in feeding control: possible function and mechanism. *Cell Mol Neurobiol*. 2008;28:469-478. https://doi.org/10.1007/s10571-007-9236-z
35. Mendoza J, Pevet P, Felder-Schmittbuhl MP, Bailly Y, Challet E. The cerebellum harbors a circadian oscillator involved in food anticipation. *The Journal of Neuroscience: The Official Journal of the Society for Neuroscience* 2010;30(5):1894–1904. Epub 2010/02/05. https://doi.org/10.1523/jneurosci.5855-09.2010. PubMed PMID: 20130198.
36. Berman SM, Paz-Filho G, Wong ML, Kohno M, Licinio J, London ED. Effects of leptin deficiency and replacement on cerebellar response to food-related cues. *Cerebellum (London, England)*. 2013;12(1):59–67. Epub 2012/05/12. doi: https://doi.org/10.1007/s12311-012-0360-z. PubMed PMID: 22576622; PubMed Central PMCID: PMCPMC3569483.
37. McTaggart JS, Lee S, Iberl M, Church C, Cox RD, Ashcroft FM. FTO is expressed in neurones throughout the brain and its expression is unaltered by fasting. *PLOS One*. 2011;6:e27968. https://doi.org/10.1371/journal.pone.0027968
38. Weise CM, Piaggi P, Reinhardt M, Chen K, Savage CR, Krakoff J, et al. The obese brain as a heritable phenotype—a combined morphometry and twin study. *International journal of obesity (2005)*. 2017;41(3):458–466. https://doi.org/10.1038/ijo.2016.222. PubMed PMID: PMC5402354.
39. Kharabian Masouleh S, Arélin K, Horstmann A, et al. Higher body mass index in older adults is associated with lower gray matter volume: implications for memory performance. *Neurobiology of Aging*. 2016;40:1-10. https://doi.org/10.1016/j.neurobiolaging.2015.12.020
40. Bauer CC, Moreno B, Gonzalez-Santos L, Concha L, Barquera S, Barrios FA. Child overweight and obesity are associated with reduced executive cognitive performance and brain alterations: a magnetic resonance imaging study in Mexican children. *Pediatr Obes* 2015;10(3):196–204. Epub 2014/07/06. https://doi.org/10.1111/ijpo.241. PubMed PMID: 24989945.
41. Janowitz D, Wittfeld K, Terock J, Freyberger HJ, Hegenscheid K, Volzke H, Habes, M., Hosten, N., Friedrich, N., Nauck, M. and Domanska, G. Association between waist circumference and gray matter volume in 2344 individuals from two adult community-based samples. *Neuroimage* 2015;122:149–157. Epub 2015/08/11. https://doi.org/10.1016/j.neuroimage.2015.07.086. PubMed PMID: 26256530.
42. Kurth F, Levitt JG, Phillips OR, et al. Relationships between gray matter, body mass index, and waist circumference in healthy adults. *Hum Brain Mapp*. 2013;34:1737-1746. https://doi.org/10.1002/hbm.22021
43. Weise CM, Thiyyagura P, Reiman EM, Chen K, Krakoff J. Fat-free body mass but not fat mass is associated with reduced gray matter volume of cortical brain regions implicated in autonomic and homeostatic regulation. *NeuroImage*. 2013;64:712–721. https://doi.org/10.1016/j.neuroimage.2012.09.005. PubMed PMID: PMC4178061.
44. Raschpichler M, Straatman K, Schroeter ML, Arelin K, Schlogl H, Fritzsch D, Mende, M., Pampel, A., Böttcher, Y., Stumvoll, M. and Villringer, A. Abdominal fat distribution and its relationship to brain changes: the differential effects of age on cerebellar structure and function: a cross-sectional, exploratory study. *BMJ open*. 2013;3(1).e001915. Epub 2013/01/29. doi: https://doi.org/10.1136/bmjopen-2012-001915. PubMed PMID: 23355665; PubMed Central PMCID: PMCPMC3563141, e001915.
45. Prehn K, Jumpertz von Schwartzenberg R, Mai K, et al. Caloric restriction in older adults—differential effects of weight loss and reduced weight on brain structure and function. *Cereb Cortex*. 2017;27:1765-1778. https://doi.org/10.1093/cercor/bhw008
46. Haltia LT, Viljanen A, Parkkola R, Kemppainen N, Rinne JO, Nuutila P, Kaasinen V Brain white matter expansion in human obesity and the recovering effect of dieting. *J Clin Endocrinol Metab* 2007;92(8):3278–3284. Epub 2007/05/31. https://doi.org/10.1210/jc.2006-2495. PubMed PMID: 17536002.
47. Verstynen TD, Weinstein AM, Schneider WW, Jakicic JM, Rofey DL, Erickson KI. Increased body mass index is associated with a global and distributed decrease in white matter microstructural integrity. *Psychosomatic medicine*. 2012;74(7):682–690. https://doi.org/10.1097/PSY.0b013e318261909c. PubMed PMID: PMC3586991.
48. Figley CR, Asem JS, Levenbaum EL, Courtney SM. Effects of body mass index and body fat percent on default mode, executive control, and salience network structure and function. *Frontiers in neuroscience*. 2016;10:234. Epub 2016/07/06. doi: https://doi.org/10.3389/fnins.2016.00234. PubMed PMID: 27378831; PubMed Central PMCID: PMCPMC4906227.
49. Contreras-Rodriguez O, Martin-Perez C, Vilar-Lopez R, Verdejo-Garcia A. Ventral and dorsal striatum networks in obesity: link to food craving and weight gain. *Biol Psychiatry* 2017;81(9):789–796. Epub 2016/01/27. https://doi.org/10.1016/j.biopsych.2015.11.020. PubMed PMID: 26809248.

50. Gautier JF, Chen K, Salbe AD, Bandy D, Pratley RE, Heiman M, Ravussin E, Reiman EM, Tataranni PA Differential brain responses to satiation in obese and lean men. *Diabetes* 2000;49(5):838–846. Epub 2000/07/25. PubMed PMID: 10905495.
51. Gearhardt AN, Yokum S, Stice E, Harris JL, Brownell KD. Relation of obesity to neural activation in response to food commercials. *Social Cognitive and Affective Neuroscience*. 2014;9(7):932–0938. https://doi.org/10.1093/scan/nst059. PubMed PMID: PMC4090951.
52. Contreras-Rodríguez O, Vilar-López R, Andrews ZB, Navas JF, Soriano-Mas C, Verdejo-García A. Altered cross-talk between the hypothalamus and non-homeostatic regions linked to obesity and difficulty to lose weight. *Scientific reports*. 2017;7(1):9951. https://doi.org/10.1038/s41598-017-09874-y. PubMed PMID: 28855582.
53. Tomasi D, Wang G-J, Wang R, Backus W, Geliebter A, Telang F, Jayne MC, Wong C, Fowler JS, Volkow ND Association of body mass and brain activation during gastric distention: implications for obesity. *PLoS ONE*. 2009;4(8):e6847. https://doi.org/10.1371/journal.pone.0006847. PubMed PMID: PMC2729391.
54. Frank S, Laharnar N, Kullmann S, et al. Processing of food pictures: influence of hunger, gender and calorie content. *Brain Research*. 2010;1350:159-166. https://doi.org/10.1016/j.brainres.2010.04.030
55. Burger KS. Frontostriatal and behavioral adaptations to daily sugar-sweetened beverage intake: a randomized controlled trial. *Am J Clin Nutr*. 2017;105(3):555–563. Epub 2017/02/10. doi: https://doi.org/10.3945/ajcn.116.140145. PubMed PMID: 28179221; PubMed Central PMCID: PMCPMC5320411.

How to cite this article: Lugo-Candelas C, Pang Y, Lee S, et al. Differences in brain structure and function in children with the *FTO* obesity-risk allele. *Obes Sci Pract*. 2020;6:409–424. https://doi.org/10.1002/osp4.417